Available online at www.sciencedirect.com
SCIENCE DIRECT®
ELSEVIER
Applied Surface Science 219 (2003) 158–166
applied surface science
www.elsevier.com/locate/apsusc

Electronic structure of the $Cu_3Au(1\ 1\ 1)$ surface

Ch.E. Lekka[a,*], N. Bernstein[b], M.J. Mehl[b], D.A. Papaconstantopoulos[a,b]

[a]*School of Computational Sciences, George Mason University, Fairfax, VA, USA*
[b]*Center for Computational Material Science, Naval Research Laboratory, Washington, DC, USA*

Abstract

Using the NRL-tight binding method, we investigate the electronic structure of the unrelaxed $Cu_3Au(1\ 1\ 1)$ surface. The tight binding parameters were determined by fitting to LDA calculations and found to reproduce the surface energy, bulk elastic constants and bulk phonon modes. The surface electronic band structure shows electronic states at the center of the Brillouin zone, within −0.1 Ry of the Fermi level, in agreement with available photoemission data. For these states, we give an interpretation and characterization of the contributions of the s, p and d electrons of the Cu and Au atoms. Charge calculations on each atom indicate that upon formation of Cu_3Au there is charge transfer from the Au atoms to the Cu atoms in agreement with previous X-ray experiments. The $Cu_3Au(1\ 1\ 1)$ surface atoms are found to gain charge compared to the bulk system, and the Au atoms regain some of the charge that they lost upon formation of bulk Cu_3Au. Despite the fact that this tight binding Hamiltonian was fitted to bulk properties of the Cu_3Au system, it is able to accurately describe the main features of the $Cu_3Au(1\ 1\ 1)$ surface, suggesting that this method is reliable for studying binary intermetallic alloy surfaces.

PACS: 71.15.F; 68.35.B; 71.20.B

Keywords: Tight binding approximation; Crystal structure of surfaces; Electronic structure of alloys

1. Introduction

The binary intermetallic alloy Cu_3Au has been the subject of numerous investigations due to its relationship with materials having improved electronic properties for technological applications including catalysis, coating, and high temperature devices [1–3]. A thorough understanding of any material requires detailed and exhaustive knowledge of its electronic structure. Theoretical [4–7] and experimental [8–11] studies established that in Cu_3Au there is hybridization of Cu and Au states giving rise to a mix of d bands, with the Au states dominating at the bottom of the d bands and the Cu at the top. Upon formation of Cu_3Au the Au 5d band is depleted [8–10], while the spatial compression of the 5d shells of Au is most likely due to the sp electrons that favor a smaller atomic volume [12]. While the situation is rather clear concerning the bulk system, studies that could give an insight on the surface electronic structure are rather limited. Angle-resolved ultraviolet photoemission spectroscopy of the $Cu_3Au(1\ 1\ 1)$ surface revealed two sp-like surface resonances at 0.4 and 1.0 eV below the Fermi energy and near the center of the surface Brillouin zone (SBZ) [13,14]. The surface state (SS) at 0.4 eV is commonly referred to as a Shockley SS and has been extensively studied in the cases of the Cu, Ag and Au (1 1 1) surfaces [15–17]. The Shockley SS has served as a

* Corresponding author. Tel.: +1-302-6510-97310; fax: +1-302-6510-97034.
E-mail address: me00110j@cc.uoi.gr (Ch.E. Lekka).

0169-4332/$ – see front matter © 2003 Published by Elsevier Science B.V.
doi:10.1016/S0169-4332(03)00592-0

prototype for the observation of a variety of phenomena [18–32] and it was found to play an important role in surface morphology [31], surface band structure [18,19,21,27–29], adsorbates and steps [32]. Therefore, a Shockley-type SS may also play a significant role in phenomena happening on the Cu_3Au surface [33–46], rendering a detailed study of this state very important. Despite its importance, detailed studies describing this state and other possible SSs, along with the contribution of the s, p and d electrons of the Au and Cu atoms are lacking.

The aim of the present work is to study the surface band structure of the $Cu_3Au(1\,1\,1)$ surface and to obtain information on the role of the s, p and d electrons of Cu and Au atoms in selected states. We used the NRL-tight binding (TB) method [47–52] in conjunction with density functional theory in the local density approximation (DFT LDA) to provide the database needed for the determination of the necessary TB parameters. The NRL-TB approach is approximately 10^3 times faster than the various LDA methods and therefore more feasible for the large number of atoms needed for surface calculations in the present work. Because of its quantum-mechanical character the NRL-TB scheme is preferable to empirical methods such as the embedded atom method (EAM). Certainly, the empirical methods produce total energies faster but the TB has more reliable transferability to structures that were not fitted. A second advantage of the quantum-mechanical basis of the TB calculations is that they yield eigenvalues and eigenvectors that allow us to evaluate charge transfer between bulk and surface atoms. We selected the $Cu_3Au(1\,1\,1)$ surface because it has the same stoichiometry as the bulk system [53] (25% Au concentration) and there is a variety of experimental data for both the order–disorder transition [54–57] and the electronic structure of the ordered [13,14] and the disordered phases [58].

2. Computational details

The total energy of the NRL-TB method is expressed as

$$E(n(r)) = \sum_{n}^{occ} \varepsilon'_n \tag{1}$$

where the sum is over the occupied states and the eigenvalues are shifted to include the non-band structure energy appearing in the DFT formalism

$$\varepsilon'_n = \varepsilon_n + \frac{F(n(r))}{N_e} \tag{2}$$

where ε_n are the Kuhn–Sham eigenvalues of the DFT calculations, N_e is the number of electrons in the calculation and $F(n(r))$ includes corrections to the kinetic energy and the Coulomb energy double counting terms. The shift $F(n(r))/N_e$ avoids the need to choose an arbitrary zero of energy for the band structure term and the usual pair-potential term, simplifying the numerical fitting process. The detailed justification is explained elsewhere [47–52].

The two-center Slater–Koster formulation of TB with a non-orthogonal basis breaks the problem into the calculation of the on-site, Hamiltonian and overlap parameters. In this method, the on-site parameters depend on the local environment and represent the energy required to place an electron in a specific atomic shell. The Hamiltonian (hopping integral) parameters represent the matrix elements for electrons hopping from one site to another and the overlap parameters describe the mixing between non-orthogonal orbitals on neighbor sites. In all three cases, we must determine pairwise interactions between atoms of the same type as well as those between atoms of different species [51]. This involves an extension of the original work, which only describes monoatomic systems [47–50,59–61].

The environmental dependence of the on-site parameters is controlled by a set of atomic-like densities [51]

$$p(i,\tilde{j}) = \sum_{j\in\tilde{j}} \exp(-\lambda^2_{\tilde{i}\tilde{j}}|R_i - R_j|)F(|R_i - R_j|) \tag{3}$$

where the ith atom is of type $\tilde{i}$; the jth atom of type $\tilde{j}$; $\rho(i,\tilde{j})$ is the density of atom i due to neighboring atoms of type $\tilde{j}$; and $\lambda_{\tilde{i}\tilde{j}}$ is a fitting constant to be determined. The cut-off function F takes the form

$$F(R) = \frac{\theta(R_c - R)}{\{1 + \exp[(R - R_c)/L_c + 5]\}} \tag{4}$$

where θ is the step function. For the Cu–Au system, we take $R_c = 12.5$ Bohr and $L_c = 0.5$ Bohr for all interactions.

The on-site terms themselves are polynomial functions of $\rho^{2/3}$

$$h_k(i) = \alpha_k(\tilde{i}) + \sum_{\tilde{j}} [b_k(\tilde{i},\tilde{j})\rho(i,\tilde{j})^{2/3} + c_k(\tilde{i},\tilde{j})\rho(i,\tilde{j})^{4/3} + d_k(\tilde{i},\tilde{j})\rho(i,\tilde{j})^2] \quad (5)$$

where the sum is over all atom types in the system. In general, we use $k = \mathrm{s}, \mathrm{p}, \mathrm{d}$.

The two-center Slater–Koster hopping integrals are determined using an exponentially damped polynomial, and depend only on the atomic species and the distances between the atoms:

$$H_{kk'\mu}(i,j;R) = [A_{kk'\mu}(\tilde{i},\tilde{j}) + B_{kk'\mu}(\tilde{i},\tilde{j})R + C_{kk'\mu}(\tilde{i},\tilde{j})R^2] \exp[-D^2_{kk'\mu}(\tilde{i},\tilde{j})R]F(R) \quad (6)$$

where the parameters A, B, C and D are to be fitted. For like-atom ($\tilde{i} = \tilde{j}$) interactions, there are 10 independent Slater–Koster parameters:

$$\mathrm{ss}\sigma, \mathrm{sp}\sigma, \mathrm{pp}\sigma, \mathrm{pp}\pi, \mathrm{sd}\sigma, \mathrm{pd}\sigma, \mathrm{pd}\pi, \mathrm{dd}\sigma, \mathrm{dd}\pi, \mathrm{dd}\delta.$$

When the atoms are of different types, we must include an additional four parameters:

$$\mathrm{ps}\sigma, \mathrm{ds}\sigma, \mathrm{dp}\sigma, \mathrm{dp}\pi.$$

Since we are using a non-orthogonal basis set, we must also parametrize the overlap integrals. These have a form similar to that of the hopping integrals

$$S_{kk'\mu}(i,j;R) = [O_{kk'\mu}(\tilde{i},\tilde{j}) + P_{kk'\mu}(\tilde{i},\tilde{j})R + Q_{kk'\mu}(\tilde{i},\tilde{j}\}R^2] \exp[-T^2_{kk'\mu}(\tilde{i},\tilde{j})R]F(R) \quad (7)$$

where O, P, Q and T also represent parameters to be fitted.

For a two-component system with s, p and d orbitals, there are 316 parameters used in the fit, in contrast to 93 for a single-element parameterization [48,51]. These parameters are chosen to reproduce the DFT LDA values of the eigenvalues $\varepsilon_n{}'$ and energies E in Eq. (1) over a variety of structures.

The basic aim of our procedure is to represent the Slater–Koster Hamiltonian using simple functional forms with the parameters chosen to reproduce the first-principles calculations over a wide range of pressure and structures. The parameters are obtained by fitting to band structures and total energies of the DFT LDA calculations. We constructed the database of electronic band structures and total energies for various structures at several volumes around the equilibrium density. In all cases, we used a uniform regular k-point mesh. For the pure Cu and Au that k-point mesh corresponds to 146, 55 and 84 k-points in the irreducible part of the face-centered cubic (fcc) lattice, body-centered cubic (bcc) lattice and the simple cubic (sc) zone, respectively. For the CuAu sodium–chloride (B_1), cesium–chloride (B_2) and copper–gold ($L1_0$) structures, we use a k-point mesh of 89, 84 and 216 k-points, respectively. In addition, we used 84 and 60 (or 44) k-points in the Cu_3Au ($L1_2$) and $AlFe_3$ (DO_3) structures for the Cu_3Au and Au_3Cu lattices, respectively. For each structure, we used 5–11 volumes, with the largest number of volumes for the experimental equilibrium structure. The total database of eigenvalues and total energies contains about 5000 entries. We used the Levenberg–Marquardt algorithm to adjust our TB parameters to give the best possible reproduction of the database. The total energies are usually weighted at about 500 times larger than a single band. We first fitted the total energies and the band structures of pure Cu (sc, bcc, fcc) and pure Au (sc, bcc, fcc) separately and fixed the corresponding parameters. We then fitted the total energies and the band structures of CuAu(B_1, B_2), Cu_3Au($L1_2$, DO_3) and Au_3Cu (($L1_2$, DO_3), in order to determine the Cu–Au interactions. For these structures, the average rms error of the occupied bands is approximately 20 mRy and less than 1 mRy for the total energies.

After obtaining the TB parameters, we validated them by calculating the equilibrium lattice constant, elastic constants and the phonon modes in the high symmetry points for bulk Cu_3Au as shown in Table 1. *In principle, the TB parameters obtained with the procedure described above are not unique. However, we find that the validation tests eliminate unsuitable parameter sets, and that remaining parameter sets give equivalent results for the properties we study here.* Then, we proceeded with the calculation of surface properties. For the $Cu_3Au(1\,1\,1)$ surface electronic structure we performed TB calculations using a 15 atomic layer slab and extended periodically in directions perpendicular to the (1 1 1) surface. By fixing the dimension of the simulation box at a value twice as large as the thickness of the crystal along the z-direction, we simulated an isolated slab.

Table 1
Bulk properties of Cu_3Au

Property	Experiment	LAPW	Present work
A (Bohr)	7.086	6.949	6.975
B (GPa)	152	140	131
C' (GPa)	52	60	100
C_{11} (GPa)	187	180	198
C_{12} (GPa)	135	120	98
C_{44} (Gpa)	68	–	92
Γ_4 (cm^{-1})	0	0	0
Γ_4 (cm^{-1})	125	110	153
Γ_4 (cm^{-1})	210	200	270
Γ_5 (cm^{-1})	161	159	195

Equilibrium lattice parameter (a), bulk modulus (B), elastic constants ($C' = C_{11} - C_{12}$, C_{11}, C_{12} and C_{44}), phonon modes at the $\bar{\Gamma}$ point (Γ_4 and Γ_5) along with the corresponding quantities found with the LAPW method and the available experimental data [59–61].

3. Results

3.1. Bulk properties

A direct result of the fitting procedure, which reproduces the total energies of the Cu_3Au system at several volumes, is an accurate determination of the equilibrium lattice parameters and the bulk modulus. In addition, we calculated the elastic constants Cu, C_{12} and C_{44} by imposing external strains in the crystal [61] and obtaining the energy as a function of strain, from the curvature of which we numerically deduce the elastic constants. Furthermore, using the frozen phonon method [47,62] we calculate the phonon modes at the center of the Brillouin zone ($\bar{\Gamma}$ point). These results are summarized in Table 1 along with the corresponding quantities found independently by the LAPW method and from available experimental data. As we can see, our predictions are in overall agreement with the LAPW results and with experimental data not only for the lattice parameter [63] and the bulk modulus which we have essentially fitted, but also for the elastic constants [64] and the phonon modes [65], which are not included in the fitting database.

The electronic density of states (DOSs) of Cu_3Au ($L1_2$) was obtained by the tetrahedron method [66], using 165 k-points in the irreducible part of the Brillouin zone. In Fig. 1, we present the total DOS

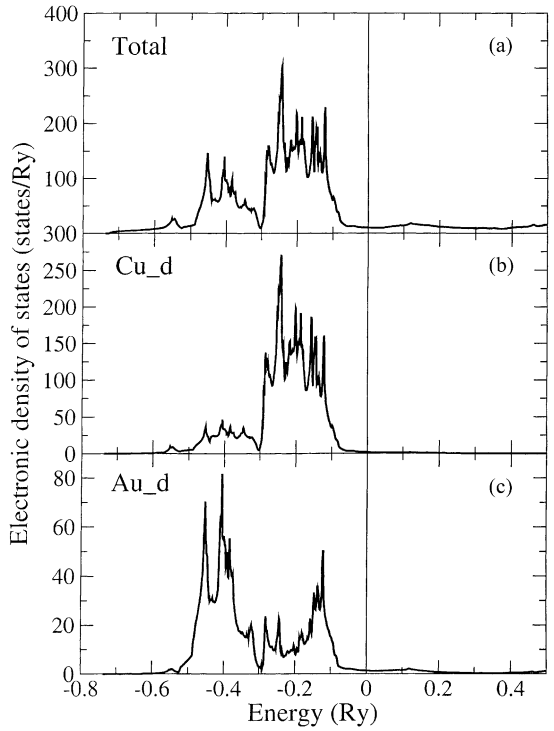

Fig. 1. Electronic density of states of the Cu_3Au: (a) total DOS, (b) d partial DOS of Cu atoms, and (c) d partial DOS of Au atoms. In each case, the Fermi level has been set to 0.

(Fig. 1a) along with the d partial DOS of Cu and Au atoms (Fig. 1b and c, respectively). We observe that below the Fermi level, the electronic states have mostly d character while above it they show mainly s and p character. In Fig. 1b and c, we see that both kinds of atoms contribute to the entire d-band energy range from −0.6 to −0.05 Ry giving rise to a common d band for the Cu_3Au system. Nevertheless, the Au d states dominate the bottom of the d band (Fig. 1c) while the contribution of the Cu d states is larger near the top (Fig. 1b). These results are in very good agreement with available theoretical [4–7] and experimental studies [8–11].

3.2. Surface energy

In order to calculate the surface energy, we evaluate the energy of the bulk Cu_3Au (E_{Cu_3Au}) and the energy of the $Cu_3Au(1\,1\,1)$ surface slab (E_s) separately for a system of 60 atoms (15 atomic layers) and

331 in-plane k-points. We evaluated the surface energy (γ) by:

$$\gamma = \frac{E_s - E_{Cu_3Au}}{2A} \quad (8)$$

where E_s is the energy of the slab with two free surfaces, E_{Cu_3Au} is the energy of the ordered Cu_3Au bulk and A is the surface area. Our calculation predicts a surface energy of 1708 and 1648 mJ/m^2 for the unrelaxed and the relaxed $Cu_3Au(1\,1\,1)$ surface, respectively. These results are consistent with our LAPW–LDA results which give 1596 mJ/m^2 for the unrelaxed surface, calculated using 28 atoms (seven atomic layers) and 14 k-points, based on the WIEN2k code [67]. The system used in the LAPW–LDA calculation is small compared to the TB calculation because it requires a lot of computational time to perform an LAPW calculation in 60 atoms and 331 k-points. Furthermore, it worth noting that the agreement of the TB calculation with the LAPW–LDA result is much better than for most empirical potentials (including some based on the second moment approximation, Finnis–Sinclair and EAM), which give values between 863 and 993 mJ/m^2 for the relaxed γ [37,38,41,43]. The potential of Bozzolo–Ferrante–Smith (BFS) is the one exception, giving a very good relaxed γ of 1577 mJ/m^2 [39,40].

3.3. Band structure

The band structures of the Cu_3Au bulk system along the $\bar{\Gamma} \rightarrow \bar{R}$ direction and the $Cu_3Au(1\,1\,1)$ surface along the $\bar{\Gamma} \rightarrow \bar{M}$ direction are depicted in Fig. 2a and b, respectively. In Fig. 2a, the narrow bands of the bulk system below the Fermi level are a mixture of the Cu and Au d bands, in agreement with available theoretical [4–7] and experimental [8–11] data, while the bands above the Fermi level have mainly s and p character (Section 3.1). The $\bar{\Gamma} \rightarrow \bar{R}$ direction of the bulk system (in k-space (1 1 1) direction), projects

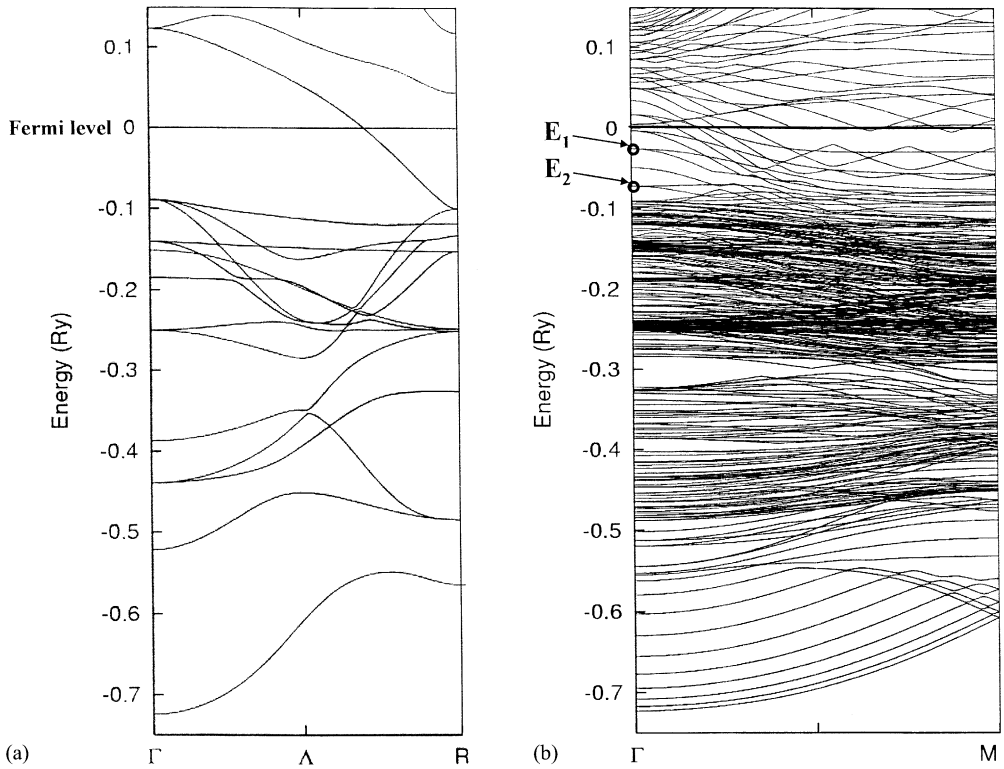

Fig. 2. Band structure of the Cu_3Au: (a) bulk system along the ΓR direction, and (b) (1 1 1) surface along the ΓM direction. E_1 and E_2 are the experimentally determined surface states.

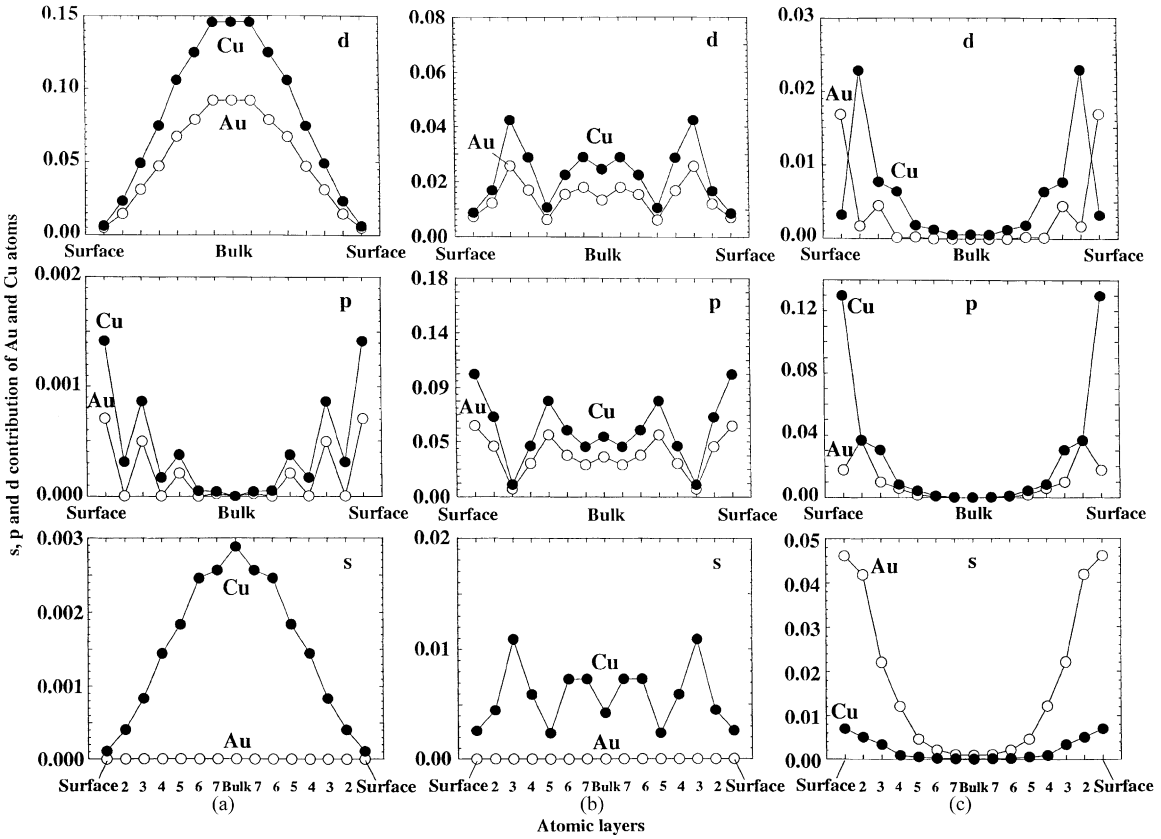

Fig. 3. Contribution of the s, p and d electrons of Cu (●) and Au (○) as a function of atomic layers for the three energy states (a) −0.090, (b) −0.026, and (c) 0.004 Ry at the center of the Brillouin zone.

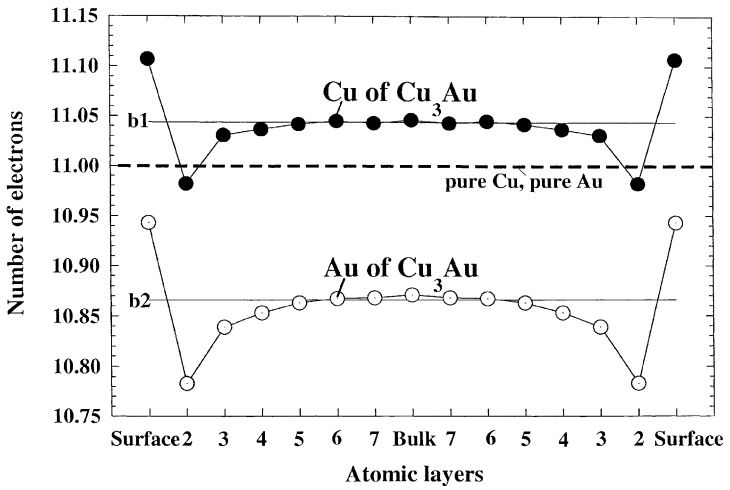

Fig. 4. Number of electrons of the Cu (●) and the Au (⊙) atoms for the different atomic layers. The dotted line (labeled pure Cu and pure Au) corresponds to the number of electrons (11 e^-) in the pure Cu and pure Au system, while the b1 and b2 lines refer to the number of electrons of the bulk Cu and bulk Au atoms in the Cu_3Au system, respectively.

onto $\bar{\Gamma}$ of the (1 1 1) SBZ. For comparison with available experimental results, we will focus our attention at the $\bar{\Gamma}$ point and close to the Fermi level. We recall here that angle-resolved photoemission spectroscopy on the Cu_3Au(1 1 1) surface shows two sp-like SSs at $E_1 = -0.029$ Ry (Shockley SS) and $E_2 = -0.073$ Ry [13]. As can be seen in Fig. 2b, in this energy region between the main d-character area (black region) and the Fermi level of the Cu_3Au(1 1 1) surface band structure there are several energy states. Two of these, at −0.026 and −0.072 Ry, lie very closely in energy to the experimental SS. With the aim of understanding whether these are SSs and obtaining information concerning the role of s, p and d electrons of Cu and Au atoms, we perform a detailed analysis of the energy states close to the Fermi level, near $\bar{\Gamma}$ of the SBZ. In Fig. 3, we present the contributions of the s, p and d electrons of the Cu (●) and Au (○) atoms as a function of the atomic layer for three states with energy of −0.090 (Fig. 3a), −0.026 (Fig. 3b) and 0.004 Ry (Fig. 3c). In the −0.090 Ry state (Fig. 3a), in the bulk the majority of the electronic contributions is due to Cu d, Au d and Cu s electrons and this contribution vanishes as we proceed towards the surface layer. In contrast, for the same energy state the role of p electrons in the bulk system is negligible but becomes important at the surface layer. The state at −0.026 Ry (very close in energy to the experimental E_1 state) cannot be clearly classified as a pure SS or a bulk state because there are significant contributions from both bulk and surface atoms. Similar behavior was also found for the state that is close to the E_2 experimental state. For the 0.004 Ry state (Fig. 3c), we observe that near the surface the contribution of the s, p and d electrons of both Au and Cu atoms is very important, while it becomes negligible when approaching the bulk, suggesting that this energy state is a pure SS.

3.4. Charge transfer

For the bulk Cu_3Au system as well as the unrelaxed Cu_3Au(1 1 1) surface, we calculate the charge on each Cu and Au atom by summing the occupied DOS projected on each atom. In Fig. 4, we plot the number of electrons of the Cu and the Au atoms for the different atomic layers of the Cu_3Au(1 1 1) surface. We observe that upon formation of Cu_3Au, the Au atoms lose -0.13 e$^-$ compared to the pure Au, while the Cu atoms gain $+0.03$ e$^-$, in agreement with XANES and XPS experimental data [8]. Turning to the surface behavior, we find that the Cu_3Au(1 1 1) surface atoms gain charge, and in particular the Au atoms regain 57% of the charge lost upon the formation of Cu_3Au.

To understand the contribution of different electronic states to the overall charge transfer, we present in Fig. 5 the decomposition of the curves in Fig. 4 into contributions from s, p and d electrons. We observe that upon formation of the Cu_3Au system, the d and p

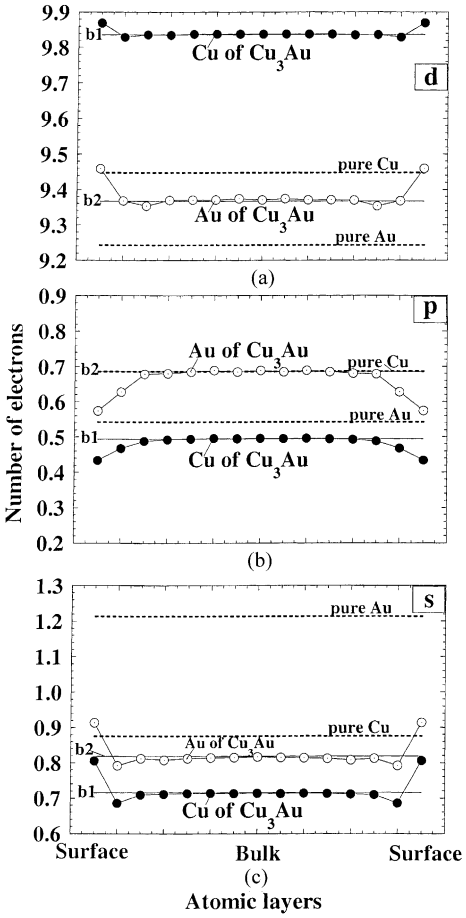

Fig. 5. Number of the d (a), p (b) and, s (c) electrons of the Cu (●) and the Au (⊙) atoms for the different atomic layers of the Cu_3Au(1 1 1) surface. The dotted line (labeled pure Cu and pure Au) corresponds to the number of electrons in the pure Cu fcc and pure Au fcc, while the b1 and b2 lines refer to the number of electrons of the bulk Cu and bulk Au atoms in the Cu_3Au system, respectively.

character of the Au bulk atoms is slightly increased while the s character is significantly decreased compared with the pure Au. The Cu atoms in Cu_3Au gain d character and loose p and s character compare to the pure Cu metal. On the surface, both Cu and Au atoms d and s orbitals gain charge while these atoms undergo a reduction of their p character compared to the Cu and Au bulk Cu_3Au atoms. It should be noted that in both Figs. 4 and 5, the numbers of electrons for the Cu and Au in the bulk region of the $Cu_3Au(1\ 1\ 1)$ slab are in very good agreement with the corresponding values for the bulk Cu_3Au system, indicating that the number of layers used in the slab calculation is sufficient and that there is no interaction between the two surfaces through the bulk.

4. Conclusions

In the present study, we investigate the electronic structure of the ordered $Cu_3Au(1\ 1\ 1)$ unrelaxed surface using the NRL-TB method. We first separately determine the TB parameters for the pure Cu and pure Au system by fitting to LDA calculations the total energy and the band structure for the fcc, bcc and sc structures. Then we fit the corresponding values for the CuAu (B_1 and B_2 structures), the Cu_3Au and Au_3Cu ($L1_2$ and DO_3 structures) in order to fix the Cu–Au interactions. We find that the our TB Hamiltonian satisfactorily reproduces the elastic constants, the bulk phonon frequencies at the high symmetry points of the $L1_2$ Cu_3Au system and the surface energy of the $Cu_3Au(1\ 1\ 1)$ system. We perform a detailed analysis on the surface electronic band structure close to the Fermi level and at the center of the Brillouin zone and we find two states situated at -0.026 and -0.072 Ry, that lie closely in energy to the SS found in photoemission experimental data. Calculation of the charge on each atom reveals that upon formation of Cu_3Au there is charge transfer from the Au atoms to the Cu atoms, in agreement with X-ray experiments. In addition, both species of the $Cu_3Au(1\ 1\ 1)$ surface gain charge compared to the bulk system, especially the Au atoms that regain most of the electron charge loss that occurs upon formation of the bulk Cu_3Au. We conclude that despite the fact that we fit the TB Hamiltonian only to bulk properties of the Cu_3Au system, it describes accurately the main features of the $Cu_3Au(1\ 1\ 1)$ surface.

Acknowledgements

We thank Dr. A. Aguayo for his help with the WIEN2k code.

References

[1] W. Pfeiler, B. Sprusil, Mater. Sci. Eng. A324 (2002) 34.
[2] T.W. Kim, D.U. Lee, D.C. Choo, Y.S. Lim, H.S. Lee, J.Y. Lee, H. Lim, Solid State Commun. 117 (2001) 501.
[3] P. Deurinck, C. Creemers, Surf. Sci. 419 (1998) 62.
[4] B. Ginatempo, G.Y. Guo, W.M. Temmerman, J.B. Staunton, P.J. Durham, Phys. Rev. B42 (1990) 2761.
[5] P. Weinberger, A.M. Boring, R.C. Albers, W.M. Temmerman, Phys. Rev. B38 (1988) 5357.
[6] H.L. Skriver, H.P. Lengekeek, Phys. Rev. B19 (1979) 900.
[7] J. Davenport, R.E. Watson, M. Weinert, Phys. Rev. B37 (1988) 9985.
[8] T.K. Sham, Y.M. Yiu, M. Kuhn, K.H. Tan, Phys. Rev. B41 (1990) 11881.
[9] G. Wertheim, L.F. Mattheiss, D.N.E. Buchanan, Phys. Rev. B38 (1988) 5988.
[10] G. Wertheim, Phys. Rev. B36 (1987) 4432.
[11] Z.Q. Wang, S.C. Wu, J. Quinn, C.K.C. Loc, Y.S. Li, F. Jona, J.W. Davenport, Phys. Rev. B38 (1988) 7442.
[12] V. Heine, L.D. Marks, Surf. Sci. 165 (1986) 65.
[13] R. Courths, M. Lau, T. Scheunemann, H. Gollish, R. Feder, Phys. Rev. B63 (2001) 195110.
[14] M. Lau, S. Loubus, R. Courths, S. Halilov, H. Gollisch, R. Feder, Ann. Physik 2 (1993) 450.
[15] S.D. Kevan, R.H. Gaylord, Phys. Rev. B36 (1987) 5809.
[16] P.O. Gartland, B.J. Slagsvold, Phys. Rev. B12 (1975) 4047.
[17] P. Heimann, H. Neddermeyer, H.F. Roloff, J. Phys. C10 (1977) L17.
[18] S.D. Kevan, Phys. Rev. Lett. 50 (1983) 526.
[19] J. Tersoff, S.D. Kevan, Phys. Rev. B28 (1983) 4267.
[20] R. Courths, H. Wern, U. Hau, B. Cord, V. Bachelier, S. Houfner, J. Phys. F: Met. Phys. 14 (1984) 1559.
[21] B.A. McDougall, T. Balasubramanian, E. Jensen, Phys. Rev. B51 (1995) 13891.
[22] S. LaShell, B.A. McDougall, F. Jensen, Phys. Rev. Lett. 77 (1996) 3419.
[23] J.A. Knapp, F.J. Himpsel, D.E. Eastman, Phys. Rev. B19 (1979) 4952.
[24] Y. Petroff, P. Thiry, Appl. Opt. 19 (1980) 3957.
[25] S.G. Louie, P. Thiry, R. Pinchaux, Y. Petroff, D. Chandesris, J. Lecante, Phys. Rev. Lett. 44 (1980) 549.
[26] T.C. Hsieh, P. John, T. Miller, T.-C. Chiang, Phys. Rev. B35 (1987) 3728.
[27] R. Matzdorf, G. Meister, A. Goldmann, Phys. Rev. B54 (14) (1996) 807.
[28] F. Theilmann, R. Matzdorf, A. Goldmann, Surf. Sci. 420 (1999) 33.
[29] G. Nicolay, F. Reinert, S. Schmidt, D. Ehm, P. Steiner, S. Houfner, Phys. Rev. B62 (2000) 1631.

[30] R. Panagio, R. Matzdorf, G. Meister, A. Goldmann, Surf. Sci. 336 (1995) 113.
[31] Th. Fauster, Ch. Reuss, I.L. Shumay, M. Weinelt, F. Theilmann, A. Goldmann, Phys. Rev. B61 (2000) 16168.
[32] L. Bourgi, L. Petersen, H. Brune, K. Kern, Surf. Sci. 447 (2000) L157.
[33] B. Gans, P.A. Knipp, D.D. Koleske, S.J. Sibener, Surf. Sci. 264 (1992) 81.
[34] D.H. Oh, H.J. Kang, K.H. Chae, C.N. Whang, B.V. King, D.J. O'Connor, D.W. Moon, Surf. Sci. 477 (2001) L289.
[35] L. Houssiau, P. Bertrand, Surf. Sci. 352 (1996) 978.
[36] S.M. Foiles, Surf. Sci. 191 (1987) 329.
[37] M. Hayoun, V. Pontikis, C. Winter, Surf. Sci. 398 (1998) 125.
[38] W.E. Wallace, G.J. Ackland, Surf. Sci. 275 (1992) 1685.
[39] R.J. Kobistek, G. Bozzolo, J. Ferrante, H. Schlosser, Surf. Sci. 307–309 (1994) 390.
[40] G. Bozzolo, J. Ferrante, R.D. Noebe, B. Good, F.S. Honecy, P. Abel, Comp. Mater. Sci. 15 (1999) 169.
[41] W. Fei, A. Kara, T. Rahman, Phys. Rev. B61 (2000) 16105.
[42] Ch.E. Lekka, N.I. Papanicolaou, G.A. Evangelakis, Surf. Sci. 479 (2001) 287.
[43] Ch.E. Lekka, N.I. Papanicolaou, G.A. Evangelakis, Surf. Sci. 488 (2001) 269.
[44] Ch.E. Lekka, G.A. Evangelakis, Surf. Sci. 473 (2001) 39.
[45] Ch.F. Lekka, D.G. Papageorgiou, G.A. Evangelakis, Surf. Sci. 518 (2002) 111.
[46] N.I. Papanicolaou, G.C. Kallinteris, G.A. Evangelakis, D.A. Papaconstantopoulos, M.J. Mehl, J. Phys. Condens. Matter 10 (1998) 10979.
[47] R.F. Cohen, M.J. Mehl, D.A. Papaconstantopoulos, Phys. Rev. B50 (1994) 14694.
[48] M.J. Mehl, D.A. Papaconstantopoulos, Phys. Rev. B54 (1996) 4519.
[49] N. Berstein, M.J. Mehl, D.A. Papaconstantopoulos, N.I. Papanicolaou, M.Z. Bazant, E. Kaxiras, Phys. Rev. B62 (2000) 4477.
[50] F. Kirchhoff, M.J. Mehl, N.I. Papanicolaou, D.A. Papaconstantopoulos, F.S. Khan, Phys. Rev. B63 (2001) 195101.
[51] S.H. Yang, M.J. Mehl, D.A. Papaconstantopoulos, M.B. Scott, J. Phys. Condens. Matter 14 (2002) 1985.
[52] H.J. Gotsis, D.A. Papaconstantopoulos, M.J. Mehl, Phys. Rev. B65 (2002) 134101.
[53] U. Bardi, Rep. Prog. Phys. 57 (1994) 939.
[54] S.W. Bonham, C.P. Flynn, Surf. Sci. 366 (1996) L760.
[55] C. Ern, W. Donner, H. Dosch, B. Adams, D. Nowikow, Phys. Rev. Lett. 85 (2001) 1926.
[56] X.-M. Zhu, R. Feidenhans'l, H. Zabel, J. Als-Nielsen, R. Du, C.P. Flynn, F. Grey, Phys. Rev. B37 (1988) 7157.
[57] Yi. Huang, M. Gajdardziska-Josifovska, J.M. Cowley, Ultramiscoscopy 57 (1995) 391.
[58] F. Arola, R.S. Rao, A. Salokative, A. Bansil, Phys. Rev. B41 (1990) 7361.
[59] M.J. Mehl, J.F. Osburn, D.A. Papaconstantopoulos, B.M. Klein, Phys. Rev. B41 (1990) 10311;
M.J. Mehl, J.F. Osburn, D.A. Papaconstantopoulos, B.M. Klein, Phys. Rev. B42 (1991) 5362.
[60] M.J. Mehl, Phys. Rev. B47 (1993) 2493.
[61] M.J. Mehl, B.M. Klein, D.A. Papaconstantopoulos, in: J.H. Westbrook, R.L. Fleischer (Eds.), Intermetallic Compounds: Principles and Applications, Wiley, London, 1994.
[62] R.M. Klein, R.E. Cohen, Phys. Rev. B45 (1992) 12405.
[63] C. Kittel, Introduction to Solid State Physics, 4th ed., Wiley, 1971.
[64] G. Simmons, H. Wang, Single Crystal Elastic Constants and Calculated Aggregate Properties: A Handbook, 2nd ed., MIT Press, Cambridge, MA, 1971.
[65] S. Katano, M. Iizumi, Y. Noda, J. Phys. F: Met. Phys. 18 (1988) 2195.
[66] O. Jepsen, O.K. Andersen, Solid State Commun. 9 (1971) 1763.
[67] P. Blaha, K. Schwarz, G. Madsen, D. Kvasnicka, J. Luitz, in: K. Schwarz (Ed.), Computer code WIEN2k. An Augmented Plane Wave and Local Orbitals Program for Calculating Crystal Properties, Technical University of Wien, Vienna, Austria.